A Cell Center Finite Volume Model for 2D Numerical Simulation of Deposition-Erosion and Transport of Suspended Sediment in Free Surface Flows

SAEED-REZA SABBAGH-YAZDI [*], BEHZAD SAIDIFAR [**]
Civil Engineering Department,
KN Toosi University of Technology,
No.1346 Valiasr
Street, 19697- Tehran
IRAN

and

NIKOS E. MASTORAKIS
Military Insitutes of University Education (ASEI)
Hellenic Naval Academy
Terma Chatzikyriakou 18539,
Piraues, GREECE

Abstract: - The details of a cell center finite volume depth-integrated free surface flow solver which solves two-dimensional advection and diffusion equation of suspended sediment in a coupled manner. The set of flow equations is shallow water equation which considers the effect of the bed topography variations. The algorithm includes a parabolic algebraic eddy viscosity model for simulation of turbulent effects. The depth integrated equation mathematically describes the variation of the sediment concentration due to the deposition-erosion phenomenon via its sink-source terms. In present algorithm, various coefficients for non-equilibrium adaptation length in the source-sink terms of clear water sediment transport formulation is tested and verified. A cell center finite volume formulation for unstructured triangular meshes is utilized with explicit time integration. In order to prevent numerical instabilities, proper artificial viscosity terms are added to the formulation, without degradation of accuracy. Validation of the suspended sediment module is accomplished through simulation of two test cases in straight channels. The first test case, presents the net sediment entrainment into the clear water from channel bed with zero sediment deposition. The second one describes the sediment deposition on the perforated channel bed with zero sediment entrainment.

Key-Words: - Deposition-Erosion, 2D Advection-Difusion of Suspended Sediment, Free Surface Flow, Cell Center Finite Volume Method, Unstructured Triangular Mesh

1 Introduction

The transport of suspended sediment is an important area of research in fluvial hydraulics. Despite intensive research, both numerical and empirical, in the last few decades, the transport mechanisms remain far from a complete physical or analytical description. In the past few decades, 2D and 3D mathematical models for sediment transportation have been developed to predict river regime and riverbed deformation due to engineering projects [21,19,15,27,10].

One of the recently proposed mathematical models for sediment transport is the one developed based on analysis of performed by Jiang et al [6]. They tested their model for net entrainment of suspended load via two-phase modeling of suspended sediment distribution in free surface flows in a straight channel. In this model, the incorporation of the additional dispersion terms predict more accurate sediment concentration distribution along the water depth but the computational cost of employing their formulations is more than using well known Rouse model. However, results of their mathematical model in the vertical direction is similar to the classical convection–diffusion equation such as the Rouse model.

In another effort, Chia et al, [7] proposed 2-D numerical model for net entrainment of suspended load in straight channel. They used the explicit finite analytic method to discretize the governing equations for water flow. In their study, the sediment transport equation is solved in an uncoupled manner. The equilibrium concentration

profile proposed by van Rijn through a simplified method was adopted in their work.

Minh et al, [13] and Wu et al, [27] developed both 2D depth-average and 3D models which consider suspended and bed-load sediment transport and bed deformation for natural rivers. The partial differential equations for the mean flow, the turbulence model and the suspended-sediment concentration were solved with extended versions of the finite-volume codes in the 2D and 3D models. Both finite-volume codes used non-staggered curvilinear regular grids. Lin and Falconer [12] simulated similar test case using their 3D models.

Zeng et al, [29] used a full 3D (non-hydrostatic) model for predicting vertical concentration distribution in straight channel with net entrainment and one with net deposition of suspended sediment. Their model solves Incompressible, Reynolds-Averaged Navier-Stokes (RANS) equations in generalized curvilinear coordinates.

Olsen [16] used a fully 3D non-hydrostatic model to predict the meandering of alluvial channels using a finite volume time-accurate solver that can employ unstructured grids.

Singh et al, 2005 [24] used fractional step approach, also known as standard split approach (Sobey [18]) to determine longitudinal concentration profile in the case of net entrainment of suspended sediment. They used Leveque [9] algorithm for solving the advection part of the equations, which uses basic upwind method and proposed several correction terms to achieve better accuracy and stability. To solve for the diffusion part of the advection diffusion sediment transport equation, a semi-implicit finite difference scheme was used in his model.

This paper focuses on the validation of the suspended sediment transport module by using efficient of a 2D hydrostatic viscous flow solver and turbulence model. The motion of the suspended sediment in the system is described by the advection-diffusion equation. The governing equations for open channel flow and sediment transport simulations is developed and discretised with cell center finite volume method.

2 Governing Equations

Because many open channel flows are shallow water problems, the effect of vertical motions is usually of insignificant magnitude. The depth integrated two-dimensional equations are generally accepted for studying the open channel hydraulics with reasonable accuracy and efficiency. The mass and momentum equations for depth-integrated two-dimensional turbulent flows in a Cartesian coordinate system are:

2.1. Flow Equations

Theoretical bases of the SWE theory may be found in Liggett [11] and Chaudhry [2]. Cunge et al [4].

The dependent flow variables in such equations are the flow depth (h) and the x and y components of the unit discharge (hu and hv), related to the corresponding vertically averaged flow velocity components (u and v).

The depth-integrated continuity and momentum equations of open-channel flow are

$$\frac{\partial h}{\partial t}+\frac{\partial hu}{\partial x}+\frac{\partial hv}{\partial y}=0 \quad (1)$$

$$\frac{\partial hu}{\partial t}+\frac{\partial}{\partial x}(hu^2)+\frac{\partial}{\partial y}(huv)=-gh\frac{\partial}{\partial x}(h+z_b)+\frac{1}{\rho_w}\frac{\partial(hT_{XX})}{\partial x}+\frac{1}{\rho_w}\frac{\partial(hT_{XY})}{\partial y}-\frac{T_{bx}}{\rho_w} \quad (2)$$

$$\frac{\partial hv}{\partial t}+\frac{\partial}{\partial x}(hvu)+\frac{\partial}{\partial y}(hv^2)=-gh\frac{\partial}{\partial y}(h+z_b)+\frac{1}{\rho_w}\frac{\partial(hT_{YX})}{\partial x}+\frac{1}{\rho_w}\frac{\partial(hT_{YY})}{\partial y}-\frac{T_{by}}{\rho_w} \quad (3)$$

where t = time; x and y =horizontal Cartesian coordinates; h=flow depth; u and v=depth-averaged flow velocities in x and y directions; z_b =bed elevation; g =gravitational acceleration; ρ_w =density of flow; T_{XX} , T_{XY} , T_{YX} , and T_{YY} =depth-averaged turbulent stresses; T_{bx} and T_{by} =bed shear stresses that are determined by $\begin{pmatrix}T_{bX}\\T_{bY}\end{pmatrix}=\rho_w c_f\begin{pmatrix}u\\v\end{pmatrix}\sqrt{u^2+v^2}$; $c_f=\frac{n^2 g}{h^{1/3}}$, in which n=Manning's roughness coefficient. The turbulent shear stresses are determined by the Boussinesq's assumption

$$T_{XX}=2\rho_w(\upsilon_t+\upsilon)\frac{\partial u}{\partial x}-\frac{2}{3}\rho_w k \quad (4)$$

$$T_{XY}=T_{YX}=\rho_w(\upsilon_t+\upsilon)\left(\frac{\partial u}{\partial y}+\frac{\partial v}{\partial x}\right) \quad (5)$$

$$T_{YY}=2\rho_w(\upsilon_t+\upsilon)\frac{\partial v}{\partial y}-\frac{2}{3}\rho_w k \quad (6)$$

Where, υ =kinematic viscosity of water; υ_t =eddy viscosity due to turbulence; and k = turbulence

energy, which is dropped from Eqs. (4) and (6) when the zero-equation turbulence models are used. Several turbulence models, including the depth-averaged parabolic eddy viscosity model, the mixing length model, the standard k-« turbulence model (Rodi, [17]), have been innovated to determine the eddy viscosity υ_t. In the present paper, only the depth-averaged parabolic model is used. In the depth-averaged parabolic model, the eddy viscosity is calculated by $\upsilon_t = \alpha_t U_* h$, in which U_*= bed shear velocity $U_* = \left[C_f (U^2 + V^2)\right]^{1/2}$ and α_t is the empirical coefficient between 0.3 and 1.0.

2.2. Mass Balance for Suspended Sediment

A two dimensional conservation form of the advection-diffusion equation for sediment transport can be written as:

$$\frac{\partial hC_K}{\partial t} + \frac{\partial uhC_K}{\partial x} + \frac{\partial vhC_K}{\partial y} = \frac{\partial}{\partial x}(k_x h \frac{\partial C_K}{\partial x}) + \frac{\partial}{\partial y}(k_y h \frac{\partial C_K}{\partial y}) + E_K - D_K \quad (7)$$

where C_K =depth-averaged concentration of the k^{th} size class of suspended load

E_K and D_K are erosion and deposition terms in upward and downward directions, respectively, and together known as source-sink term in the advection-diffusion equation. The source-sink term can be calculated as $E_K - D_K = S = \alpha w_{sk}(C_{*k} - C_k)$; and w_{sk} =settling velocity of sediment particles with k^{th} size.

k_x, k_y =diffusivity coefficient of sediment in *x* and *y* directions there are related to the turbulent eddy viscosity [23]. $k_x = k_y = \upsilon_t / \sigma_t$ the turbulent eddy viscosity in the horizontal direction was assumed to be constant, σ_t is turbulent Prandtl-Schmidt number (value between 0.5 and 1.0).

A formula for sediment concentration close to bed has to include only local bed parameters: sediment characteristics, bed shear stress and turbulence. Van Rijn [21] used dimensionless numbers of shear stress and particle diameter to correlate empirical coefficients against observations from the field and flume experiments. According to his method, the boundary condition at the bed for the convection-diffusion equation can be specified by specifying an equilibrium sediment concentration close to bed. This approach is most used today and given as: $C_{*k} = 0.015 d_{50} T^{1.5} / \delta_b D_*^{0.3}$ where the particle-size diameter $D_* = d_{50}\left[(\rho_s - \rho)g/\rho\upsilon^2\right]^{1/3}$ and the non-dimensional excess bed shear stress $T = \left[(u_*')^2 - (u_{*cr})^2\right] / (u_{*cr})^2$. In these relations, d_{50}= median diameter of the bed material, ρ_s= density of this material, ρ = density of water, u_*'= effective bed shear velocity related to the grain and u_{*cr} = critical bed shear velocity for sediment motion given by Iwagaki [5]:

$$u_{*cr} = \sqrt{a\left(d_m / 10\right)^b} \quad (8)$$

Where, a, *b=constants; a=0.0226, b=1* for $d_m \le 0.065mm$; *a=0.000841, b=11/32* for $0.065 < d_m \le 0.565mm$; *a=0.0055, b=1* for $0.565 < d_m \le 1.18mm$; *a=0.01346, b=31/22* for $1.18 < d_m \le 3.03mm$; and *a=0.00809, b=1* for $d_m > 3.03mm$.

δ_b is a reference level set equal to *0.05h* [14].

The transport of suspended particles in the vertical direction for 2D uniform open channel flows is expressed as [22]:

$$\frac{c(y)}{c_*(\delta_a)} = \left(\frac{h-y}{y}\frac{\delta_a}{h-\delta_a}\right)^z \quad \text{and} \quad z = \frac{w}{\beta' k u_*} \quad (9)$$

The fall velocity of the particles is denoted *w*, *k* is constant equal to *0.4*, water depth is denoted *h*, *y* is the distance from the bed where the reference concentration $c_*(\delta_a)$ is taken.

β' describes the difference in the diffusion of a sediment particle from the diffusion of a fluid 'particle'. The coefficient β' is calculated as: $\beta' = 1 + 2(w/u_*)^2 \quad for \quad 0.1 < w/u_* < 1$

W.H. Graf, M. Cellino [26] studied the experimental determination of the depth-averaged β' value, given by the ratio of the sediment, and the momentum, diffusion coefficients. Theirs study explained In the case of suspension flows over a movable bed without bed forms the measured β' values at capacity condition are smaller than unity,. $\beta' < 1$ However, it also was shown that for flows over a movable bed with bed forms the β' values are larger than unity, $\beta' > 1$.

2.2.1. Non-Equilibrium Adaptation Coefficient α

The non-equilibrium adaptation coefficient α is also assigned different values by different

investigators in their studies. Han et al. (1980) and Wu and Li (1992) used $\alpha = 1$ for strong erosion $\alpha = 0.25$ for strong deposition and $\alpha = 0.5$ for weak erosion and deposition. Yang (1998)[28] used a very small value *0.001* for α Thus, the non-equilibrium adaptation coefficient α. is also defined as a user-defined parameter in the model. In the model $\alpha = 0.006$ was taken to achieve the best results.

2.2.2. Near Bed Shear Velocity

There are many ways in hydraulics to evaluate the shear velocity on the channel bed; the method that described in here is adopted in the current model. The method is to calculate shear the velocity $U_* = \left[C_f (U^2 + V^2)\right]^{1/2}$ as well as the shear stress $T = \left[(u_*')^2 - (u_{*cr})^2\right] \Big/ (u_{*cr})^2$ on the bed surface is to utilize the Manning's coefficient. The shear velocity is conveniently computed by:

$$u_*^2 = \frac{\tau}{\rho} = \frac{1}{\rho}\sqrt{\tau_{bx}^2 + \tau_{by}^2} \tag{10}$$

Using above that can account for roughness effects is used to simply equate u_*' to u_*.

The Manning's coefficient n is a local constant, which does not change with the flow condition, this approach is more efficient for practical applications because it is easier to lump the effects of bed form, channel geometry, sediment size and vegetation, etc. It is important that when loose bed and bank are considered (with or without sediment in motion), the roughness height k_s and Manning's n used for calculating shear stress should include both bed material grain size and bed form roughness effects. These two parameters representing bed resistance to the flow can be converted from each other using Strickler's formula: $n = k_s^{\frac{1}{6}} \Big/ A$.

The value of parameter *A* is in the neighborhood of *20* depending on the sediment size, bed form, vegetation, and channel morphology. The effective roughness is computed as:

$$k_s = 3D_{90} + 1.1\Delta\left(1 - e^{\frac{25\Delta}{\lambda}}\right) \tag{11}$$

where λ is bed form length, calculated as $7.3d$ where d is the water depth and Δ is the bed form height, an example of a bed form predictor is given by van Rijn [21] estimating the bed form height, Δ. Equation (11) developed based on uniform sediment size variations.

$$\frac{\Delta}{h} = 0.11\left(\frac{D_{50}}{h}\right)^{0.3}\left(1 - e^{\left[\frac{u_*^2 - u_{*cr}^2}{2u_{*cr}^2}\right]}\right)\left(25 - \left[\frac{u_*^2 - u_{*cr}^2}{u_{*cr}^2}\right]\right) \tag{12}$$

3 Numerical Formulation

An important factor in applying numerical techniques is the question of grid generation.

An unstructured triangular mesh has been deployed to cover the solution domain and enable arbitrary and complex geometries to be replicated.

In a finite volume cell centre scheme, each triangle is considered as a control volume and the state variables are located at its centroid, so that the number of unknown vectors is the same as the number of cells or triangles.

For prevention of interpolating from the same derivatives on the centroid nodes located on two sides of the edge in stretched cells, nearly non-stretched triangular meshes are used

The shallow water equations written in conservation form. One of the more common forms of the equations encountered within the literature is written as:

$$U = \begin{bmatrix} h & hu & hv & hc \end{bmatrix}^T \tag{13}$$

$$\frac{\partial U}{\partial t} + \nabla \cdot F = S \tag{14}$$

Where $F = F(U) = \left[E(U), G(U)\right]$ is the flux vector and S is the source term as:

$$E = \begin{bmatrix} hu \\ hu^2 + g\dfrac{h^2}{2} \\ huv \\ huc \end{bmatrix}, \quad G = \begin{bmatrix} hv \\ huv \\ hv^2 + g\dfrac{h^2}{2} \\ hvc \end{bmatrix}, \tag{15}$$

$$S_0 = \begin{bmatrix} 0 \\ -ghS_{0x} - c_f u\sqrt{u^2 + v^2} + \upsilon_t \nabla^2 uh \\ -ghS_{0x} - c_f v\sqrt{u^2 + v^2} + \upsilon_t \nabla^2 vh \\ \dfrac{\partial}{\partial x}(k_x h\,\partial c/\partial x) + \dfrac{\partial}{\partial y}(k_y h\,\partial c/\partial y) + \alpha w_s (c_{*\delta a} - c) \end{bmatrix}$$

The bottom slope in *x* and *y* directions is indicated with S_{0x} and S_{0y}, g is the gravitational acceleration.

The finite volume method is based on writing the mathematical model equations in integral form over a control volume. In this work any triangular cell of the mesh is considered as a control volume is.

The continuity, momentum and the advection-diffusion equations are integrated over each triangular control volume as,

$$\int_{\Omega}\frac{\partial U}{\partial t}dx.dy+\int_{\Omega}\nabla\cdot F dx.dy=\int_{\Omega}S.dv \qquad (16)$$

By application of the Green's theorem to the integrated continuity and momentum equation the discrete form of the above equation is obtained as,

$$U^{n+1}=U^{n}-\frac{\Delta t}{\Omega}\left[\sum_{i=1}^{3}(\overline{E}\cdot\Delta y-\overline{G}\cdot\Delta x\right]+S\cdot\Delta t \qquad (17)$$

Where U^n is the known value of U at computational stage of n, while U^{n+1} is the value of U to be computed after computational time step Δt. Here Ω_i is the area of the control volume. The fluxes $\overline{E}$ and $\overline{G}$ are the averaged values of the fluxes in x and y spatial derivatives which are computed as functions of U^n. These fluxes are calculated in centre of boundary edges of the triangular shape control volumes by averaging of the fluxes computed at two cells adjacent to both sides of the desired edge (Figure 1).

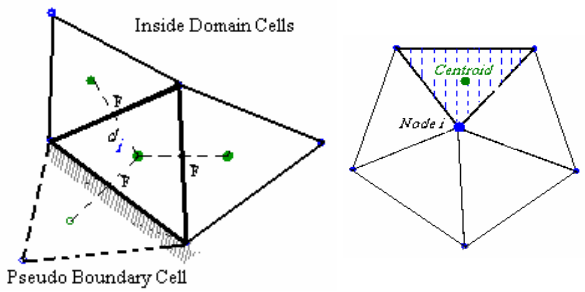

Fig. 1. Weighted averaging stencil, left: at centroids, right: at nodal points

However, for computation of the average fluxes $\overline{E}$ and $\overline{G}$ at the boundary cells, it is assumed that there is another pseudo cell out side the computational domain (with the same values of E and G at its centre) adjacent to boundary cell. S is the known values of parameters in right hand of equation.2 and equal to zero for continuity equation.

The integral discretisation of the flux through the whole surface boundary of the control volume is obtained by performing the summation, over the tree sides of each triangular cell.

For the above mentioned numerical scheme, before proceeding to the next time-step, the imposed values at boundary nodes should be transferred to the cell centroid. Hence, all boundary values are updated using following weighted averaging, which its weighting coefficient is proportional to the distance of the neighboring nodes from the desired cell centroid (Figure 1).

$$(U_i)_{Cell\,Centroid}=\frac{(U_i)_{Node}/d_i}{\sum_{i=1}^{3}1/d_i} \qquad (18)$$

Therefore, prior to this computation, it is necessary to update the flow variables ($U=[h\quad hu\quad hv\quad hc]^T$) at interior node of the boundary cell. This updating can be completed by application of following relation.

$$(U_i)_{Cell\ Node}=\frac{\Omega_i\,(U_i)_{Cell\,Centroid}}{\sum_{i=1}^{M}\Omega_i} \qquad (19)$$

Here, Ω_i is the area of i^{th} cell connected to the inside domain node of the boundary cell an average of the four vertices parameters, weighted with the distances between each vertices and the centroid, is used.

At the first time step the values of variable ($U=[h\quad hu\quad hv\quad hc]^T$) are assumed at cell centroids as initial condition. However, at the end of computations, in order to prepare the result for the visualization packages, the computed values of flow variables should be transported from the cell centroids to the nodal points using the relation (19).

3.1. Artificial Viscosity

In order to stabilize the explicit solution procedure by damping out the numerical oscillations, a biharmonic artificial viscosity formulation can be added to above formulation. Considering the convictive fluxes as, $C(U_i)=\sum_{i=1}^{3}(\overline{E}\cdot\Delta y-\overline{G}\cdot\Delta x)$ the fourth order artificial dissipation term, $D(U_i)=\varepsilon\sum_{j=1}^{3}\lambda_{ij}(\nabla^2U_j-\nabla^2U_i)$ can be added to the aforementioned algebraic formulation. The scaling factor λ_{ij} is computed using the maximum central values of λ at the centre of neighbor cells that connected to the centre of the i control volume. λ is evaluated by $\lambda=\left|\vec{U}.\hat{n}\right|+\sqrt{\left|\vec{U}.\hat{n}\right|^2+C^2\left(\Delta x^2+\Delta y^2\right)}$, where $C=\sqrt{g\bar{h}}$ wit g is the gravity acceleration. Here, $\vec{U}$ is average central computed velocity at two neighbor cells that are common in edge for example edge a-b in Fig 1 and $\hat{n}$ is normal vectors at boundary edges of control volume Ω, respectively result in $\vec{U}.\hat{n}=\left|\bar{u}\Delta y-\bar{v}\Delta x\right|$. Depending on the sizes of grid spacing, the coefficient of the artificial dissipation term, ε should be tuned to the minimum

required value ($1/256 \le \varepsilon \le 3/256$) for the applied mesh.

The algorithm for computation of artificial dissipation term is adopted for the unstructured meshes. Here, the Laplacian operator at every cell centers i, $\nabla^2 U_i = \sum_{j=1}^{3} (U_j - U_i)$, is computed using the variables W at two centre of all cells that are neighbor to cell's i. The maximum number of neighbor cells are tree and for boundary cells assumed another cell is available in other hand of boundary line and have same value of W according to boundary cell. The revised formula, which preserves the accuracy of the numerical solution, is written in the following form (Jameson 1981).

$$U_i^{n+1} = U_i^n - \frac{\Delta t}{\Omega_i}[C(U_i) - D(U_i)] + S_i \Delta t \quad (20)$$

For reducing computational efforts, the biharmonic operator can computed in some certain computational stages, but its value added to the discretized formulation in all computational steps.

3.2. Time Stepping

For every control volume, Ω in computational domain, the time marching limit is specified as:

$$\Delta t = (CFL)\frac{\Omega}{\lambda} \quad (21)$$

Where, parameter λ represents the maximum central values of Eigen values of Jacobin matrix at the total centre of neighbour cells that connected to the centre of the i control volume and Ω is the control volume's area. The Courant-Fredrish-Levy number (coefficient CFL) is evaluated by the stability condition for explicit computation procedure. Since we are dealing with unstructured meshes, the size of control volumes varies over the computational domain. Therefore, every control volume has its own time step, Δt.

Kleb, Batina and Williams [8] presented a local time stepping technique for the Euler and Navier-Stokes equations on unstructured meshes.

The method was demonstrated through model validation, when supercritical to sub-critical flow transition problem is considered. Results for this test are in good agreements with experimental.

3.3. Boundary and Initial Conditions

For the complete definition of the model is necessary to define the following boundary conditions:

For internal sub-critical flows distinction between inflow and outflow boundaries may prevent computational conflicts. Following implementations are made at inflow and outflow boundaries.

At inflow boundary nodes, the components of the free stream velocity, *u*, *v* and *c* are specified the inflow sediments flux is generally unknown and the depth, *h*, is extrapolated from the inside domain.

At the outflow boundary nodes, the depth, *h*, is imposed and the velocity components, *u*, *v* and *c* are extrapolated from the interior nodes of domain [1].

For wall boundary, free slip condition is implemented by setting the component of the velocity normal to the wall boundary equal to zero. $(U.\hat{n})_w = 0$ in which U is velocity component vectors and $\hat{n}$ is the normal vector perpendicular to the wall boundary. At bottom boundary conditions bed friction is considered and the concentration at the reference level c_a is locally equal to the value assumed in an equilibrium condition $c_*(\delta_a)$

4 Model Validation

Comparisons of the simulated results against experimental data for vertical distribution of suspended sediment concentration in the case of net sediment entrainment and longitudinal concentration profile in channels with net deposition are used to show the accuracy of the developed model.

4.1. Case 1: Development of Concentration Profile with clear water inflow at the upstream boundary

The experiment reported by van Rijn [20] is the typical cases to study the development of sediment concentration profiles in the downstream channel, A net sediment entrainment from the loose bed into suspension was observed at all test sections. The channel had *30 m* length, *0.5 m* width, and *0.7 m* height.

In the experiment, the water depth was *H = 0.25 m* at the upstream and the mean velocity was *U=0.67 m/s*. The bed material consisted of sand with D_{50}*=0.23 mm* and D_{90}*=0.32 mm*. The reference level δ_a is set to be *0.05h* according to that specified by Olsen [14]. The representative particle size for determining the fall velocity was chosen equal to *0.23 mm*. The corresponding fall velocity was *0.0237 m/s* and its obtained from the semi-empirical formulation of Cheng [3] for calculating sediment settling velocity from the effective diameter of the suspended sediment

$$w_s = \frac{\upsilon}{D_{50}}\left(\sqrt{25 + 1.2D_*^2} - 5\right)^{1.5} \quad (22)$$

In which D_{50} is particle diameter for *50%* finer of bed material, D_* is the dimensionless grain size that described above. At the inlet section (*x/H=0.0*) the concentration *C* was set equal to zero.

The coefficient of the sediment source/sink term calibrated to achieve the best numerical results. The simulated results at four locations measured from (*x/h=4.0* to *x/h=40.0*) are shown in Fig. (2) and compared with the measured concentration profiles. It can be observed, the present model under non-equilibrium condition successfully computes acceptable results at all downstream stations.

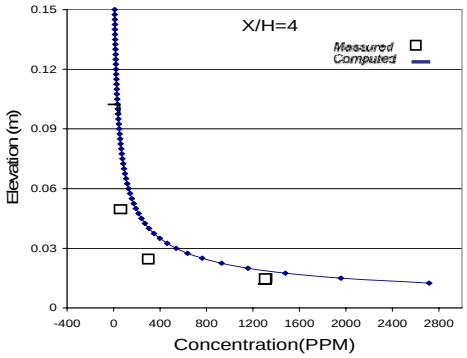

Fig. 2.a. Computed and measured suspended sediment for net entrainment at x/H=10

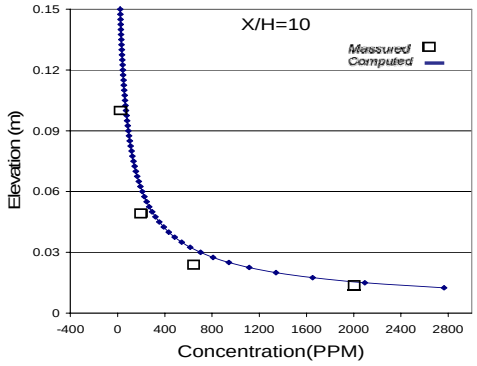

Fig. 2.b. Computed and measured suspended sediment for net entrainment at x/H=10

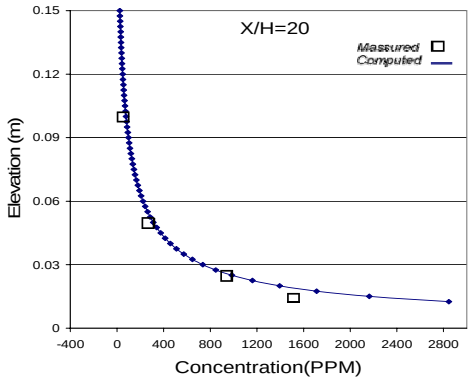

Fig. 2.c. Computed and measured suspended sediment for net entrainment at x/H=20

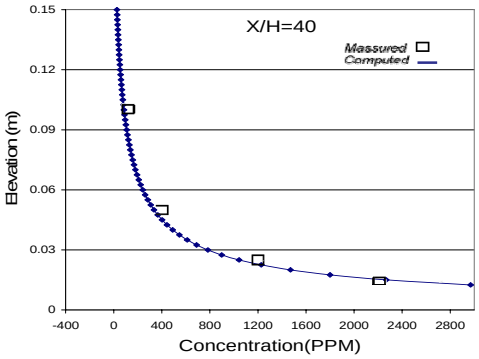

Fig. 2.d. Computed and measured suspended sediment for net entrainment at x/H=40

4.2. Case 2: Flow in a straight channel with net deposition of suspended load.

The laboratory flume a set of experimental measurement is used which is performed in aa special flume of *30m* long, *0.5m* wide and *0.5* deep (Figure 3) [25].

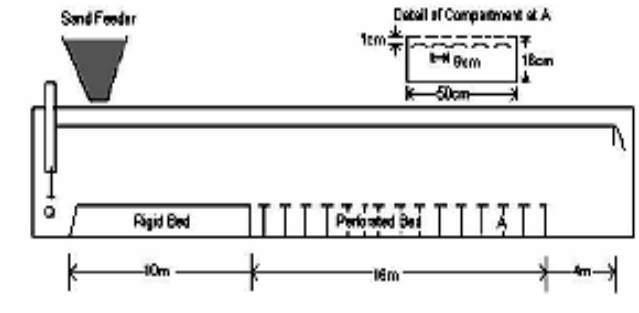

Fig. 2. Experimental setup [25]

The flume was divided into three sections. The first section was the inflow section with a rigid bed of 10m length. The second section was test section with perforated bed of 16m length and outflow of section of 4m length. The test section was made up perforated plates to avoid erosion. In order to make sure for no flow development in the chamber below perforated plates, the chamber was subdivided in compartments of 0.5m length and width equal to the flume. Rigid bed was given artificial bed roughness equal to the perforated bed roughness to minimize the change in flow conditions due to bed change from rigid to perforated bed. Sediment concentration was measured by a sediment sampler which was able to take 8 samples at a cross section in vertical direction simultaneously. The depth average sediment concentration was calculated using those 8 samples. So, over the test section there is a net deposition of suspended load. The mean velocity

was $U = 0.56\ m/s$ and the water depth $H=0.215\ m$. The characteristic diameters of the sediment material were $D_{50} = 0.1\ mm$, and $D_{90}= 0.105\ mm$. Settling velocity measured by Wang during experiment was *0.7cm/sec*.

For achieving best result, the fall velocity is computed considered by relation (22). Using this relation for w_s the value of *0.732cm/sec* is obtained.

Computed suspended sediment concentration along the flume (by using two different values for α the coefficient sediment source/sink term) is compared with reported measured values. As can be seen, the computed results are in good agreements with the concentration distribution

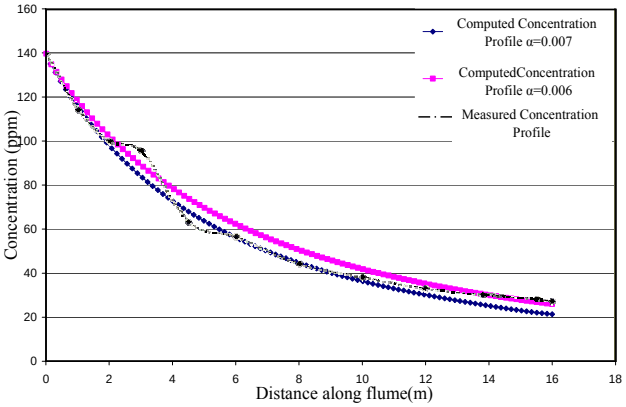

Fig. 3. Comparison between measured and computed sediment concentration along the flume

5 Conclusion

Numerical experiments are performed by developing a flow solver for modeling of sediment transport in non-equilibrium condition. The algorithm is based on solving the depth averaged flow equation by a cell-centre finite volume method on unstructured meshes.

Two simulation cases in straight open channels, with and without net sediment entrainment with reported laboratory measurements are utilized for investigation of the quality of the numerical results. However, from the sediment erosion and deposition, there is sensitivity in non equilibrium adaptation coefficient α (in source/sink term of the suspended sediment convection/diffusion equation). However, by tuning and calibration of this parameter, the satisfactory agreements between the computed and experimental were achieved. In present model $\alpha = 0.006$ was taken to achieve the best results. A comparison between analytical solution data and numerical results, obtained with a cell center finite volume algorithm, is presented.

References:

[1] Chaudhry, M. H.& Younus M., A Depth Averaged $k-\varepsilon$ Turbulence Model for the Computation of Free Surface Flow, *Journal of Hydraulic Research*, Vol 32, 1994, No.3, PP. 415-444.

[2] Chaudhry, M.H., *Open-Channel Flow*, Prentice-Hall, Inc (1993).

[3] Cheng, N.S., (1997), Simplified settling velocity formula for sediment particle, *Journal of Hydraulic Engineering ASCE, 123, 149-152.*

[4] Cunge J. Holly F and Verwey A, *Practical aspect hydraulics*, Pitman Publishing Ltd, 1980

[5] Iwagaki, Y. (1956). ,Study on critical tractive force., *Proc., JSCE, 41,1–21 (in Japanese).*

[6] Jiang J., Law A. W. K.. and Cheng N.Sh., Two-phase modeling of suspended sediment distribution in open channel flows, *Journal of Hydraulic Research Vol. 42, No. 3 (2004), pp. 273–281*

[7] Yeh K.C. and Hsu C.T., Depth-averaged modeling for channel degradation and aggradation, *National Chiao Tung Univ.*

[8] Kleb W L, Btina J T and Williams M H, Temporal adaptive Euler/Navier Stokes algorithm involving unstructured dynamic meshes, *AIAA Journal 30, 8, 1980-1985,1992*

[9] Leveque J. R. (1996), High resolution conservative algorithm for advection in incompressible flow, *Journal of numerical analysis, vol.33, no.2, pp. 627-665*

[10] Lu Yongjun, Dou Guoren, Han Longxi, Shao Xuejun, 3D Mathematical Model for Suspended Load Transport by Turbulent Flows and its Applications, *Science in China Ser. E, 2004, 47(2): 237-256*

[11] Liggett, J.A, *Fluid Mechanics*, McGraw-Hill, Inc (1994).

[12] Lin B. and Falconer R. A. 1996, Numerical modeling of three-dimensional suspended sediment for estuarine and coastal waters, *J. Hydr. Res., IAHR, 34(4): 435-456*

[13] Minh Duc, B., Wenka, Th., Rodi, W. (1998), Depth-average numerical modeling of flow and sediment transport in the Elbe river, *Proc. 3rd Int. Conf. on Hydro-science and Engineering, Cottbus/Berlin.*

[14] Nils Reidar B. Olsen, *Hydro-informatics, Fluvial Hydraulics and Limnology*, Department of Hydraulic and Environmental Engineering, 4th edition, 27 September 2004. The Norwegian University of Science and Technology.

[15] Olsen, N. R. B. (1999), Two-dimensional numerical modeling of flushing processes in water reservoirs, *J. Hydraul. Res., 37(1), 3–16.*

[16] Olsen, N.R. 2003, 3D CFD modeling of self-forming meandering channel, *J. Hydraulic Engineering, ASCE, 129(5), 366-372.*

[17] Rodi, W. (1993), Turbulence models and their application in hydraulics, 3rd Ed., *IAHR Monograph, Balkema, Rotterdam, The Netherlands.*

[18] Sobey R. J.(1983), Fraction step algorithm for estuarine mass transport, Int. *Journal of numerical methods in fluids, Vol.3, pp. 749-772*

[19] Spasojevic, M., and Holly, F. M., Jr, 2-D bed evolution in natural watercourses—New simulation approach, *J. Water., Port, Coastal, Ocean Eng., 116(4), 425–443(1990).*

[20] van Rijn, L. C. 1981, Entrainment of fine sediment particles; development of concentration profiles in a steady, uniform flow without initial sediment load, *Rep. No M1531, Part II, Delft Hydraulic Lab., Delft, The Netherlands.*

[21] Van Rijn. L. C.(1987), Mathematical modeling of morphological processes in the case of suspended sediment transport, *Ph.D Thesis, Delft university of Technology No. 382*

[22] Van Rijn LC. 1989, Sediment transport by currents and waves, *Technical Report H461. Delft Hydraulics: Delft, The Netherlands.*

[23] van Rijn, L.C., 1993, Principles of Sediment Transport in Rivers, *Estuaries and Coastal Seas, Aqua Publications, Amsterdam, The Netherlands.*

[24] Vikas Singh B.Tech., Banaras Hindu(May 2005), *Two dimensional sediment transport model using parallel computers*, MSc. Thesis Submitted to the Graduate Faculty of the Louisiana State University and Agricultural and Mechanical College.

[25] Wang Z. B. and Ribberink J. S. (1986), The validity of a depth integrated model for suspended sediment transport, *Journal of hydraulic research, IAHR, vol.24 no.1, pp. 53-67*

[26] Graf W.H., Cellino M., Suspension flows in open channels; experimental study, *Journal of hydraulic research, vol. 40, 2002, no. 4*

[27] Wu W., Rodi, W., Wenka, Th. (2000), 3D numerical modeling of flow and sediment transport in open channels, *ASCE J. Hydraulic Eng., Vol. 126, pp. 4-15.*

[28] Yang C. T., Trevino M.A. and Simoes F. J. M. (1998), User manual for GSTARS 2.0 (Generalized stream tube model for alluvial river simulation version 2.0), Sedimentation and river hydraulics group, *Technical service center, Bureau of reclamation, U. S. department of the Interior, Denver, Colarado, USA*

[29] Zeng, J., Constantinescu, G. & Weber, L. 2005, A fully 3D non-hydrostatic model for prediction of flow, sediment transport and bed morphology in open channels, *XXXIst International Association Hydraulic Research Congress, Seoul, Korea, September 2005.*